JOURNAL OF AIRCRAFT
Vol. 41, No. 3, May–June 2004

Usefulness of Transonic Model Static Data in Predicting Flight Abrupt-Wing-Stall

John E. Lamar,* Robert M. Hall,* Francis J. Capone,† and S. Naomi McMillin†
NASA Langley Research Center, Hampton, Virginia 23681

An approach is provided to answer the question of whether one can rely solely on static data taken during a transonic model test to provide the certainty needed that a new aircraft will or will not have abrupt wing stall (AWS) events during its flight operations. By the comparison of traditional static figures of merit (FOMs) with the free-to-roll (FTR) response data, a rational basis for assessing the merits of using standard testing techniques for the prediction of AWS events has been established. With use of the FTR response data as a standard, because these results compare well with flight, it is concluded that traditional FOMs can not be trusted to provide an indication as to whether a configuration will or will not have AWS tendencies. Even though these FOMs may flag features that have a high degree of correlation with the FTR response data, there are as many or more of these FOM flagged features that do not correlate. Thus, one needs to use the FTR rig to assess AWS tendencies on new configurations.

Nomenclature

C_L	=	lift coefficient
$C_{L\alpha}$	=	lift curve slope
C_l	=	rolling moment coefficient
$C_{l,\text{rms}}$	=	root mean square of the C_l
C_N	=	normal force coefficient
$C_{N,\text{rms}}$	=	root mean square of the C_N
C_{WRBM}	=	wing root-bending moment coefficient
$C_{\text{WRBM,rms}}$	=	root mean square of the C_{WRBM}
M	=	Mach number
Rn	=	Reynolds number 10^6/ft
α	=	angle of attack, deg
β	=	angle of sideslip, deg
θ	=	pitch–strut angle, deg

Subscripts

R, L	=	right or left wing

Introduction

NATURALLY occurring flight asymmetries on starboard and port wings associated with small but fixed geometrical differences, control-surface-deflection differences about the centerline, or onset flow differences normally do not give rise to significant, unplanned rolling motions with just a small change in angle of attack. Instead, these asymmetries are resisted by particular aircraft aerodynamic stability derivatives, primarily dihedral effect and damping in roll. However, for some aircraft and flight-condition combinations, the asymmetries are large and develop from an abrupt stall on one wing. This abrupt wing stall (AWS) can lead to rolling moments and, consequently, wing drop, wing rock, or other undesirable lateral stability phenomenon[1] during high subsonic or transonic maneuvers, typically a wind-up-turn.

The preceding AWS events can also be described in two other ways. First, it may be defined as an asymmetric airflow across the wings that produces an unanticipated rolling moment resulting in a lateral dynamic response of the aircraft. Moreover, the abruptness of the stall event on one wing during these maneuvers occurs with no apparent change in lateral stick. Second it may be defined as " . . . an uncommanded motion seen by the pilot as a divergence in roll and incipient departure. Typically the roll rates are not high, being of the order of 10°–20°/sec. It is clearly beyond both the aiming limit and the tactical maneuvering limit, and immediate recovery action is required in order to maintain full control."[2,3] Many production aircraft, mostly fighters, have had an asymmetrical-lift problem in which separated flow develops on one wing but remains attached on the other.[1]

The latest U.S. fighter airplane to have such phenomenon is the preproduction version of the F/A-18E/F aircraft with wing drop at transonic speeds. Another airplane still in the inventory that also has developed AWS is the AV-8B at the extremes of its operating envelope. These facts led the AWS program wind-tunnel test team to develop a plan for testing four models, the preceding two plus the F/A-18C and the F-16C, in the NASA Langley Research Center 16 Foot Transonic Tunnel (16FTT) at $M < 1$. The latter two were chosen because these aircraft do not demonstrate AWS events in flight. Hence, one goal of this testing was to look for differences in the model static measurements, or figures of merit (FOM), that would provide insight or an indication of why these two groups of aircraft have different, lateral flight characteristics.

Correlations are sought between the various potential FOM and free-to-roll (FTR)[4] or available flight response data to assess reliability of the proposed FOMs. A part of this study is to establish whether there is at least one FOM that is a necessary and sufficient condition for AWS events. If the answer to this is no, then is there one FOM that is at least a necessary condition for AWS. To accomplish the preceding aim, this paper documents various potential FOMs from static wind-tunnel tests and examines the extent to which they have proven useful in the prediction of AWS events at high subsonic and transonic speeds for these four aircraft models by comparing with the FTR response data.

Data are reported in this paper for sample combinations of flap set and Mach number for the four configurations tested without regard to whether the flaps are on schedule. Even though the aircraft flap schedules were available to the authors for these models, such knowledge will not be known to an aerodynamicist for a new airplane model before the test; hence, this reporting can be considered as a blind test. As a result, the data collected on many of the tested flap-set and Mach number combinations are for conditions the studied aircraft will never fly.

To obtain approval for releasing this paper to the public, quantitative information has been removed from most vertical scales as per guidelines from the Department of Defense.

Presented as Paper 2003-0745 at the AIAA 41st Aerospace Sciences Meeting and Exhibit, Reno, NV, 6 January 2003; received 30 May 2003; revision received 4 November 2003; accepted for publication 6 November 2003.

*Aerospace Engineer, Configuration Aerodynamics Branch. Associate Fellow AIAA.
†Aerospace Engineer, Configuration Aerodynamics Branch.

Traditional FOM Background

Background

The traditional FOM (TFOM) from static wind-tunnel tests include the lift curve break, denoted by either the C_L vs α curve or the $C_{L\alpha}$ slope change, and the C_l, $C_{l,\text{rms}}$, C_{WRBM}, and $C_{\text{WRBM,rms}}$ curves vs α. Experience has taught that changes in these parameters can be indicative of changes in the flow topology that can lead to the kinds of aircraft response denoted as AWS flight events. A discussion of each parameter group follows.

C_L *Versus* α *or* $C_{L\alpha}$ *Slope Change*

Unlike a transport aircraft wing that has basically a linear lift curve followed by a break in the curve near $C_{L,\max}$, a fighter aircraft may have multiple breaks in its lift curve associated with the redistribution of lift between the main wing and the leading-edge extension for F/A-18 E (LEX). At low values of α, the flow on the main wing is attached and the LEX produces very little vortical flow and lift due to the small incidence angle. However, with increasing α, the main wing outer panel begins to stall and the LEX vortex begins to develop more lift over itself as well as over that part of the wing behind it. The redistribution of lift at transonic speeds is further complicated by unsteady flow[5,6] produced by the varying amounts of separation, especially shock-induced, associated with Mach number and flap changes.

Any discontinuities in the slope of the lift (normal-force) curve reflect changes in the flow physics and may be indicative of a problem area buffet onset, wing drop, wing rock, or loss of roll damping. This is supported by Ref. 7, where whether lift beyond the kink "is usable" for nonlinear curves was questioned. Hence, the manner in which the actual flow transitions from the two flow topologies of predominately wing-attached flow to predominately wing-outer-panel-separated-and-LEX-vortex is critical as to whether wing drop or AWS may be expected to occur.

Figure 1a shows the kinds of C_L vs α or $C_{L\alpha}$ slope changes typical of an AWS event.

C_l *and* $C_{l,rms}$

The rationale for considering asymmetries in rolling moment is that uncommanded lateral motions are the result in flight of one wing stalling before the other. Thus, this stall feature may be captured in the tunnel by examining rolling moments[8] for nominally $\beta = 0$ deg. The moments may produce either positive or negative values depending on which wing stalls. (A previous test for the preproduction F/A-18E model (16FTT-523) has established that C_l has a transonic Mach number dependency at $\beta = 0$ deg.) However, if the model experiences lateral dynamics, then the time-averaged result of rolling moment may be small even though instantaneous values are large. On the other hand, one would expect variance, or rms, of the signal to grow. Figure 1b shows steady (time averaged, 50 samples total, 10 samples/s for 5 s) and unsteady (rms) rolling moments that can occur during AWS events. Large amplitude excursions of C_l over a limited α range are associated with a wing-drop event. By contrast, C_l sinusoidal envelope excursions with time at a fixed α are more indicative of wing rock. Because this paper focuses on static- and not time-dependent data, the C_l characteristic sought in the measured results will be that associated with wing drop.

The characteristic shape associated with AWS for the $C_{l,\text{rms}}$ is a rapid rise and then a decrease (an envelope excursion), but the ending level is higher than that at the beginning.

C_{WRBM} *and* $C_{WRBM,rms}$

The rationale of using wing root-bending moment slope changes is that it produces similar changes to the lift or normal force curves except that it is directly measuring a rolling moment at the location of the gauge. In other words, it is measuring not only a sense of the lift increase or loss, but also whether this increase or loss is inboard or outboard.

Figure 1c shows typical steady and unsteady (rms), wing root-bending moments. From previous studies done with these parameters, three conclusions follow: 1) Wing bending more readily illustrates breaks in the lift, or normal force, than does the six-component balance information for lift or normal force. 2) Breaks in the wing-bending moment curve, positive or negative, appear to be a potential FOM, although how much break does it take to trigger wing drop remains to be determined. 3) Onset of the rms excursion (as seen by an envelope) in wing root-bending moment is another good correlator with trends seen in both other tunnel parameters and flight.

Background Summary

Sudden or rapid variations in the preceding curves with α are due to flow topology changes occurring on one or both wings. These changes include flow transitions from the predominately wing-attached flow to predominately shock-induced-separated, unsteady, wing-outer-panel and an LEX vortex. The data curves are also affected by flow conditions for which the flow separates from the lower surface of an overdeflected leading-edge flap. A correlation of the impact of these flow changes, as measured by static data and evaluated via the response of the FTR rig, follows.

Approach

There are two main elements in the approach to compare the FTR response data with static wind-tunnel results. The first is that the FTR data are considered to be the standard because they compare favorably with flight.[9,10] Moreover, these data are considered here to be a reliable indicator of AWS flight events for $\alpha \geq 6$ deg. The FTR–FOM parameter[9,10] for AWS events yielded the following results: No significant activity is denoted as a green box, moderate activity is denoted as a yellow box, and severe activity is denoted as a red box. A partial sample is given in Fig. 2.

There are two consequences noted. They are as follows:

1) Noticeable FTR activity, or an AWS event, occurs at the α for which there is an associated red- or yellow-filled cell.

2) AWS events may happen at a single value of α or cover an α range.

The second element deals with agreement between the data sets. A static parameter and an AWS event are said to have agreement if the

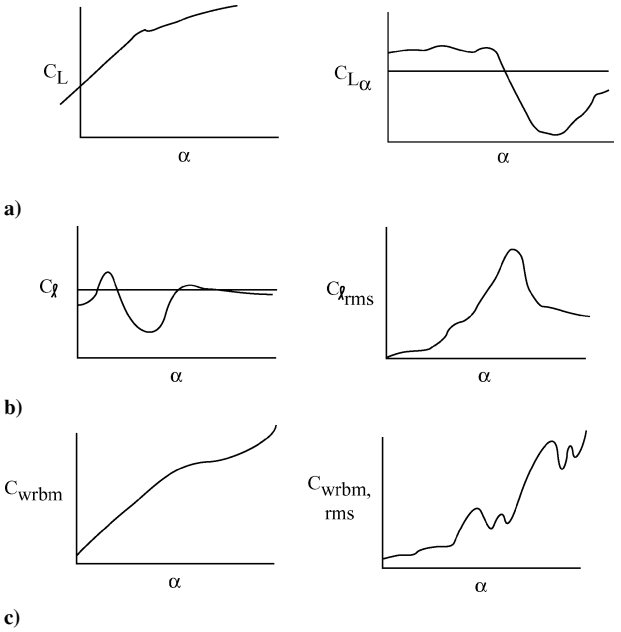

Fig. 1 Static aerodynamic coefficients that could indicate AWS events.

FTR-FOM					
θ, degrees	11.5	12.0	12.5	13.0	14.0

Fig. 2 Sample FTR–FOM results with pitch–strut angle $\theta \approx \alpha$.

α associated with any portion of the parameter break (for C_L, $C_{L\alpha,}$ and $C_{\text{WRBM,}}$) or an excursion envelope (for C_l, $C_{l,\text{rms}}$, and $C_{\text{WRBM,rms}}$) occurs within 1 deg of the α for an event. (A static-data feature, that is, break or envelope excursion that is historically characteristic of an AWS event in that TFOM, is called a flag in this paper.)

Static TFOM and FTR Data Comparisons

This section presents basic graphical comparisons of the static and FTR response data. Response data are denoted by arrows, which have been color-coded according to Fig. 2 and are plotted at the values of α for which AWS events occur. No green arrows are plotted because we seek to highlight the correlations with AWS events, not nonevents.

Before data-set comparisons were undertaken, there was a tendency to discount many small slope changes or data excursions as being within the measurement accuracy. However, after the observation that many arrow sets occurred in these same α regions, slope changes (parameter break) of any significance were counted. (Unfortunately, it is not possible to establish a direct correlation between an AWS event and a quantifiable threshold for a TFOM change that

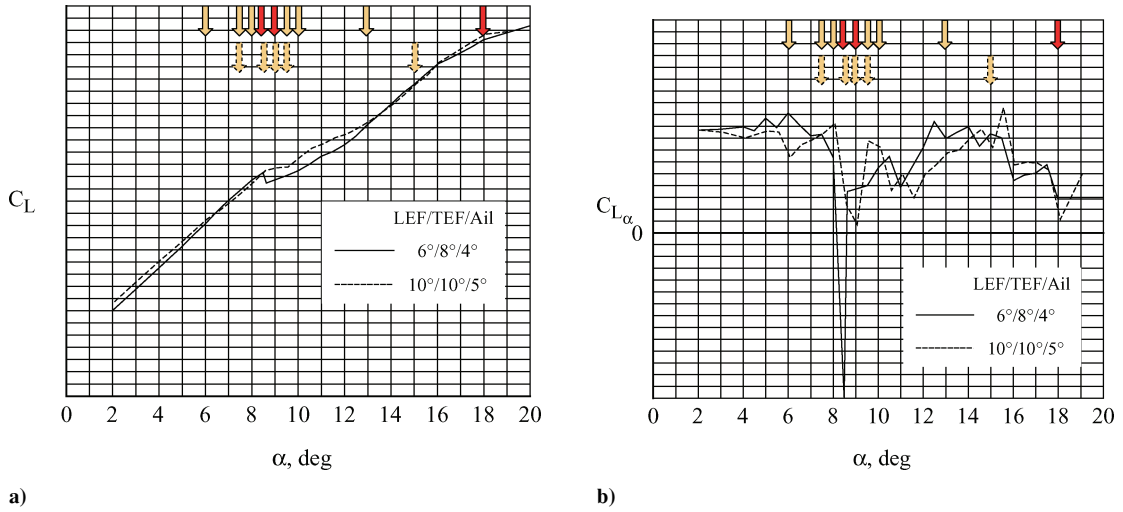

Fig. 3 Preproduction F/A-18E at $M = 0.9$: a) lift curve and b) lift curve slope.

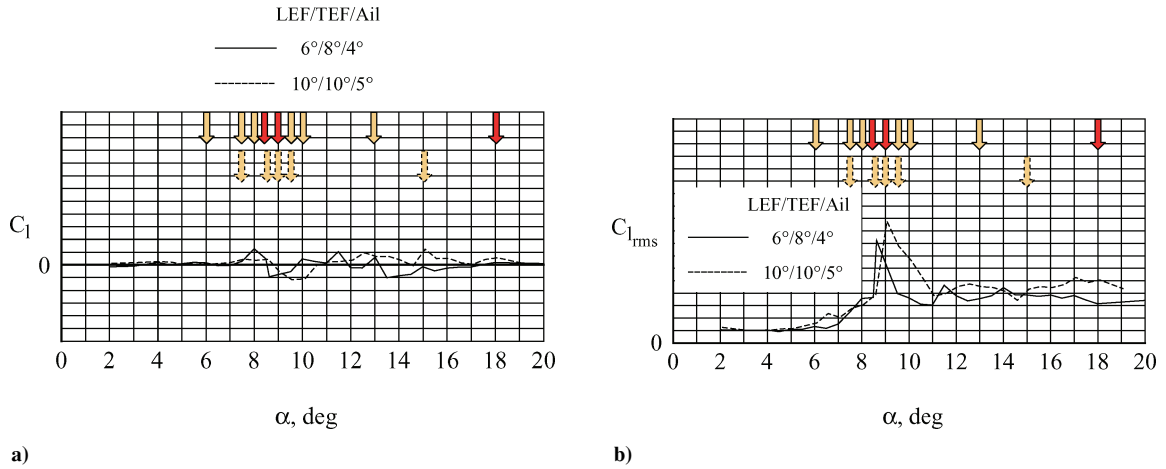

Fig. 4 Preproduction F/A-18E at $M = 0.9$: a) C_l vs α and b) $C_{l,\text{rms}}$ vs α.

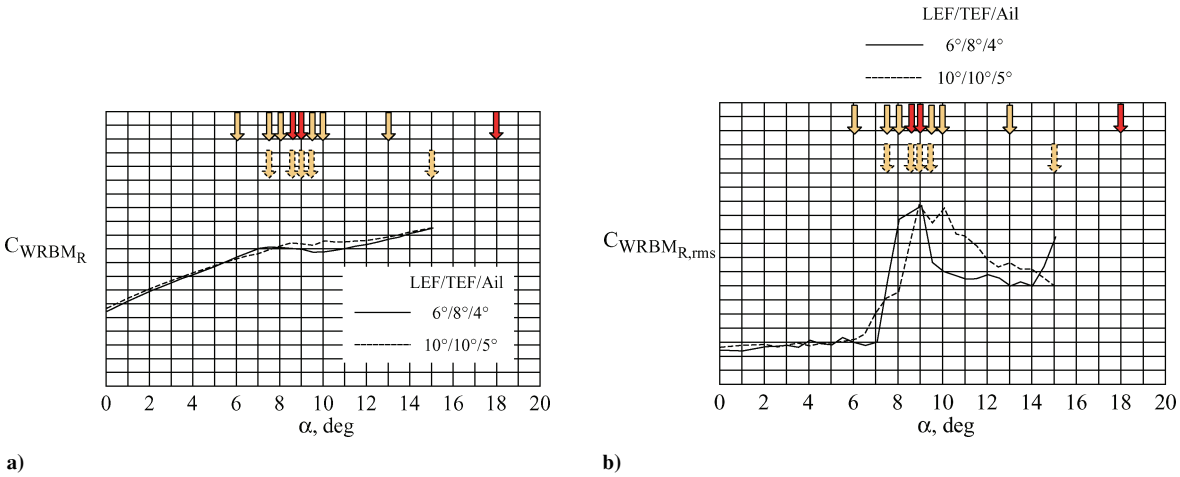

Fig. 5 Right wing root-bending-moment results for preproduction F/A-18E at $M = 0.9$ from 16FTT-523: a) $C_{\text{WRBM},R}$ vs α and b) $C_{\text{WRBM,Rrms}}$ vs α.

is generally applicable.) The preceding statement is of importance because the vertical scales on the TFOM graphs are the same for all four configurations and were not adjusted for each configuration, parameter, flap set, or Mach number. Finally, the authors have made an attempt to apply the guidance provided in the background section in performing these comparisons; however, even with the best intentions this process has been conducted subjectively and has an estimated flagged-feature count accuracy of ± 1 per curve. A large part of the subjectivity is directly related to determining how much of a TFOM change is sufficient for a feature to be flagged and counted.

Examples and Scoring

To acquaint the reader with the technique employed for assessing agreement between the two data types, an example of each basic plot and an explanation of how the agreement was scored is given for each curve. Scores for all TFOM parameters are summarized in Tables 1 and 2.

Table 1 Ratings of traditional FOM for all four models at all test conditions

LE, degs	TE, degs	Ail, degs	C_L[a]	$C_{L\alpha}$[a]	C_l[a]	$C_{l,\mathrm{rms}}$[a]	C_{WRBM}[a]	$C_{\mathrm{WRBM,rms}}$[a]
				F/A-18E, M = 0.9				
6	8	4	9(1)/9	9(2)/9	9(2)/9	8(0)/9	7(0)/9	8(0)/9
10	10	5	5(2)/5	5(5)/5	5(2)/5	5(2)/5	4(0)/5	4(0)/5
15	10	5	7(3)/7	7(6)/7	7(2)/7	7(1)/7	N/A	N/A
20	10	0	4(4)/4	4(8)/4	4(0)/4	4(0)/4	N/A	N/A
				F/A-18E, M = 0.8				
6	8	4	9(2)/9	9(5)/9	7(0)/9	9(0)/9	9(1)/9	9(1)/9
10	10	5	3(3)/3	3(7)/3	1(3)/3	3(1)/3	3(2)/3	3(1)/3
15	10	5	2(5)/2	2(7)/2	2(4)/2	2(1)/2	N/A	N/A
20	10	0	5(2)/5	5(6)/5	5(1)/5	5(1)/5	N/A	N/A
				AV-8B, M = 0.75				
*****	10[b]	*****	6(2)/6[b]	6(2)/6[b]	6(1)/6[b]	6(0)/6[b]	N/A	N/A
*****	10[c]	*****	11(1)/11[c]	11(2)/11[c]	11(0)/11[c]	11(0)/11[c]	N/A	N/A
				AV-8B, M = 0.50				
*****	25[b]	*****	0(3)/1[b]	0(3)/1[b]	1(1)/1[b]	1(1)/1[b]	N/A	N/A
*****	15	*****	0(4)/0	0(3)/0	0(0)/0	0(1)/0	N/A	N/A
*****	10	*****	0(4)/0	0(3)/0	0(0)/0	0(0)/0	N/A	N/A
*****	25[c]	*****	7(3)/7[c]	7(7)/7[c]	7(2)/7[c]	7(1)/7[c]	N/A	N/A
*****	10	*****	1(2)/1	1(1)/1	1(2)/1	1(1)/1	N/A	N/A
				AV-8B, M = 0.30				
*****	25[b]	*****	6(3)/6[b]	6(4)/6[b]	6(2)/6[b]	6(0)/6[b]	N/A	N/A
*****	25[c]	*****	10(2)/10[c]	10(2)/10[c]	10(2)/10[c]	10(0)/10[c]	N/A	N/A
				F/A-18C, M = 0.9				
0	0	0	6(1)/7	7(4)/7	7(1)/7	7(1)/7	N/A	N/A
6	8	0	2(2)/2	2(4)/2	2(3)/2	2(2)/2	N/A	N/A
10	12	0	4(4)/4	2(7)/4	4(0)/4	4(1)/4	N/A	N/A
15	12	0	1(5)/1	1(6)/1	1(3)/1	1(2)/1	N/A	N/A
				F/A-18C, M = 0.85				
0	0	0	8(0)/8	8(5)/8	4(0)/8	8(0)/8	N/A	N/A
6	8	0	7(3)/7	7(4)/7	7(1)/7	7(1)/7	N/A	N/A
10	12	0	2(3)/2	2(6)/2	2(3)/2	1(2)/2	N/A	N/A
15	12	0	2(2)/2	2(3)/2	2(1)/2	0(1)/2	N/A	N/A
				F/A-18C, M = 0.8				
0	0	0	2(2)/2	2(0)/2	2(0)/2	2(0)/2	N/A	N/A
6	8	0	7(4)/7	7(5)/7	7(0)/7	5(1)/7	N/A	N/A
10	12	0	3(6)/3	3(5)/3	3(0)/3	3(1)/3	N/A	N/A
15	12	0	2(4)/2	2(6)/2	1(1)/2	2(1)/2	N/A	N/A
				F-16C, M = 0.9				
0	0	*****	0(4)/0	0(6)/0	0(2)/0	0(1)/0	0(4)/0	0(1)/0
5	0	*****	0(4)/0	0(5)/0	0(2)/0	0(2)/0	0(4)/0	0(1)/0
10	0	*****	0(5)/0	0(4)/0	0(0)/0	0(2)/0	0(4)/0	0(1)/0
15	0	*****	0(4)/0	0(3)/0	0(0)/0	0(1)/0	0(3)/0	0(0)/0
				F-16C, M = 0.8				
0	0	*****	0(4)/0	0(6)/0	0(2)/0	0(2)/0	0(5)/0	0(1)/0
5	0	*****	0(3)/0	0(6)/0	0(0)/0	0(0)/0	0(3)/0	0(0)/0
10	0	*****	2(2)/2	2(4)/2	0(0)/2	1(1)/2	2(2)/2	1(0)/2
15	0	*****	0(3)/0	0(3)/0	0(0)/0	0(1)/0	0(3)/0	0(1)/0

[a]Pattern is xx(yy)/zz, where xx is the number of arrows within 1 deg angle of attack of an event, yy is the number of static events not indicate by arrows, and zz is the number of red and yellow arrows. [b]100% LERX. [c]65% LERX.

Table 2 Traditional FOM ratings summary by configuration

Configuration	C_L[a]	$C_{L\alpha}$[a]	C_l[a]	$C_{l,\mathrm{rms}}$[a]	C_{WRBM}[a]	$C_{\mathrm{WRBM,rms}}$[a]
F/A-18E	44(22)/44	44(46)/44	40(14)/44	43(6)/44	23(3)/26	24(2)/26
AV-8B	41(24)/42	41(27)/42	42(10)/42	42(4)/42	N/A	N/A
F/A-18C	46(36)/47	45(65)/47	42(13)/47	42(13)/47	N/A	N/A
F-16C	2(29)/2	2(37)/2	0(6)/2	1(10)/2	2(28)2	1(5)/2

[a]Pattern is xx(yy)zz where xx is the number of arrows within 1 deg angle of attack AOA of an event yy is the number of static events not indicated by arrows zz is the number of red and yellow arrows.

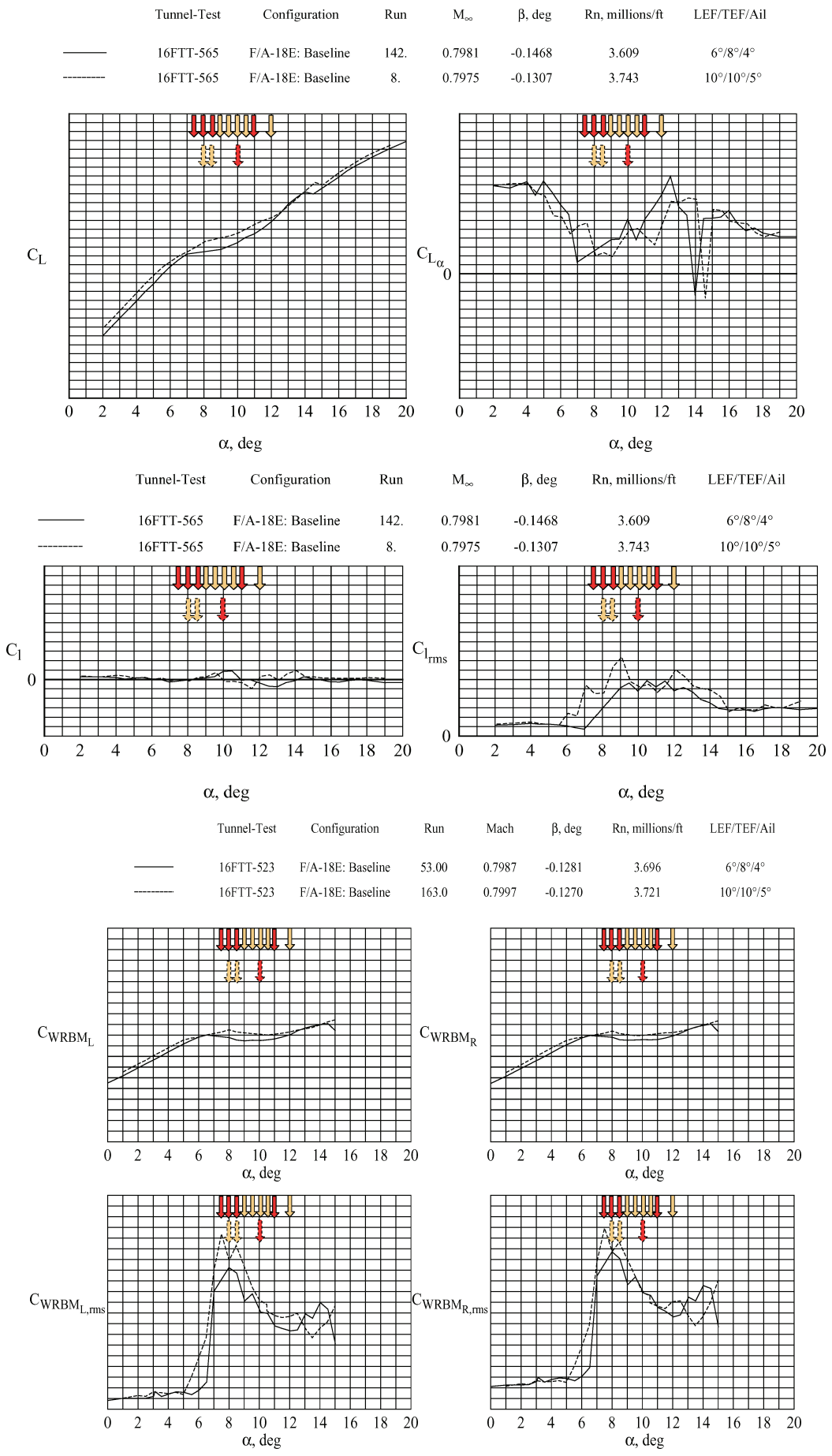

Fig. 6 Lift, rolling- and wing root-bending-moments with FTR data for the F/A-18E preproduction aircraft model at various flap settings and $M = 0.8$; LEF/TEF/Ail at 6/8/4 and 10/10/5 deg.

Application of TFOM Criterion

The criterion for agreement between the static and the FTR response data has been given in the "Approach" section. This is applied to the data and reported in the following manner as a score: The denominator is the sum of red and yellow arrows; the numerator is the number of matches between the two data sets, FTR events and static-data flagged features of breaks in curves or envelope excursions, for each TFOM; and the parenthetical number denotes the count of flags for which there was no FTR–FOM arrow within 1 deg of α. The latter are called misses. Figures 3–5 show red and/or yellow arrows associated with each curve. Note that the arrow outline is solid or dashed signifying the curve to which it belongs.

C_L *Versus* α *or* $C_{L\alpha}$ *Slope Change*

The C_L TFOM in Fig. 3a shows the solid curve to have sharp, or rapid, slope changes at values of α of 6, 8.5, 10.5, 12.5, 13, 16, and 18 deg. All nine arrows fall within 1 deg of a slope change, and so we have agreement or a score of 9 out of 9. However, at $\alpha = 16$ deg there is a slope change (flag) with no corresponding event or arrow. Hence, the score for this curve is 9(1)/9. The dashed curve has changes at values of α of 8.5, 9.5, 10.5, 13, 16, and 18 deg, which produces agreement with five events or arrows and two misses (values of α of 13 and 18 deg) for a score of 5(2)/5.

The $C_{L\alpha}$ TFOM in Fig. 3b shows the solid curve to have multiple changes, some large and others not so large. They occur at values of α of 6, 8, 8.5, 9, 9.5, 11, 12.5, 13, 15.5, 16, 17.5, and 18 deg. All nine arrows have agreement, but there are two misses (values of α of 15.5 and 16 deg), and so the score for this curve is 9(2)/9. The dashed curve has changes at values of α of 6, 8, 9, 9.5, 10.5, 11, 11.5, 15.5, 16, 17.5, and 18 deg. All five arrows have agreement, but there are five misses (values of α of 6, 11, 11.5, 17.5, and 18 deg), yielding a score of 5(5)/5.

C_l *and* $C_{l,rms}$

The C_l TFOM in Fig. 4a shows the solid curve to have AWS characteristics for values of α from 7 to 10.5 deg, at 11.5 deg, and from 12.5 to 15 deg. Nine arrows fall within 1 deg of an event, but two flags (at values of α of 11.5 and 15 deg) are missed, so the score for this curve is 9(2)/9. The dashed curve has changes for values of α from 7.5 to 11 deg and from 12.5 to 16 deg, which produces agreement with five arrows and two misses (flags at values of α of 12.5 and 18 deg) for a score of 5(2)/5.

The $C_{l,\mathrm{rms}}$ TFOM in Fig. 4b shows the solid curve to have AWS characteristics for values of α from 7 to 10 deg from 11 to 14 deg. Eight arrows have agreement and no misses, and so the score for this curve is 8(0)/9. The dashed curve has AWS characteristics from 6 to 11 deg, from 11.5 to 14.5 deg, and from 15 to 19 deg. Five of the arrows have agreement with two misses (flags at values of α of 13 and 17 deg), yielding a score of 5(2)/5.

C_{WRBM} *, and* $C_{WRBM,rms}$

The $C_{\mathrm{WRBM},R}$ TFOM in Fig. 5a shows the solid curve to have AWS characteristics at values of α of 6, 8, and 10 deg. (Because of test techniques and procedures, the α limit for this test was $\approx$ 15 deg.) Seven arrows fall within 1 deg of a flag, and none are missed, and so the score for this curve is 7(0)/9. The dashed curve has slope changes

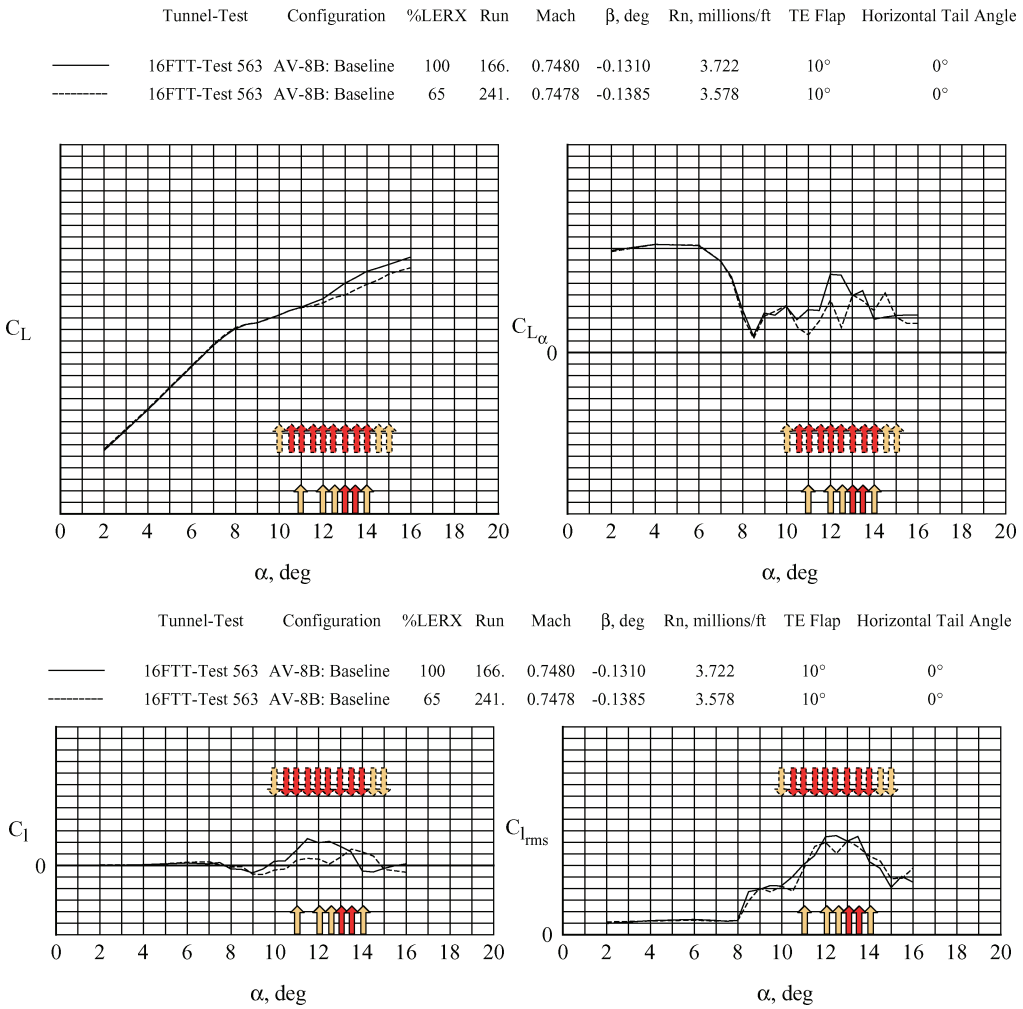

Fig. 7 Lift and rolling moments with FTR data for AV-8B aircraft model at TEF = 10 deg and $M = 0.75$; leading-edge root extention LERX = 100% and 65%.

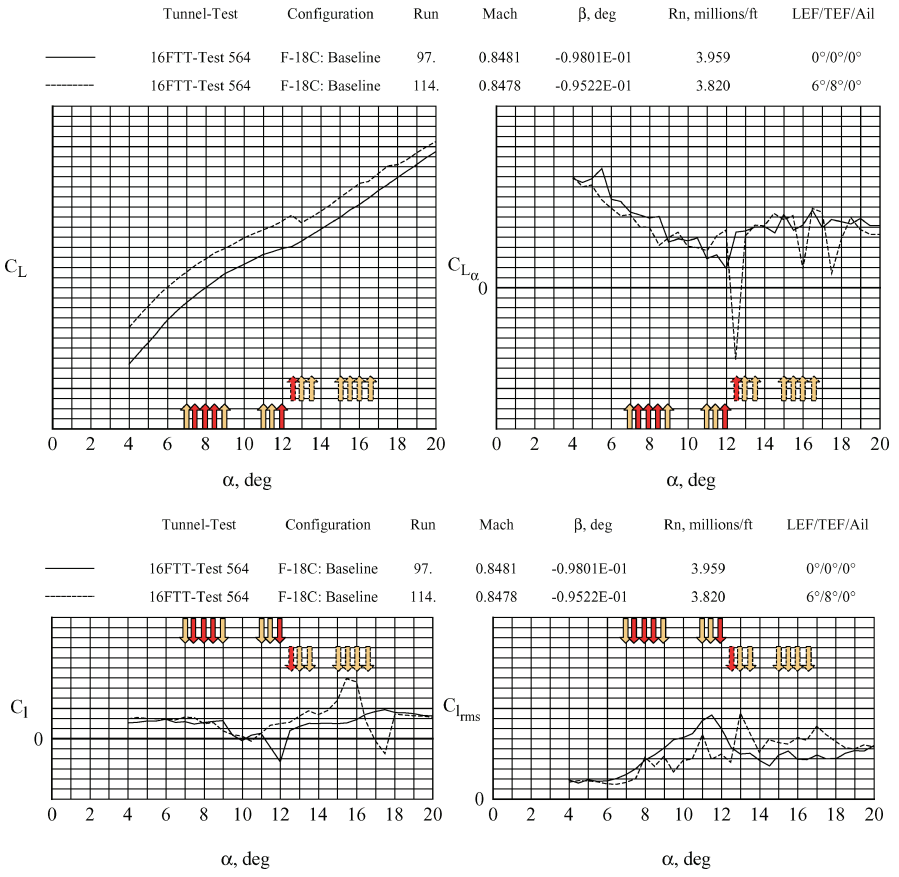

a) LEF/TEF/Ail at 0/0/0 and 6/8/0 deg

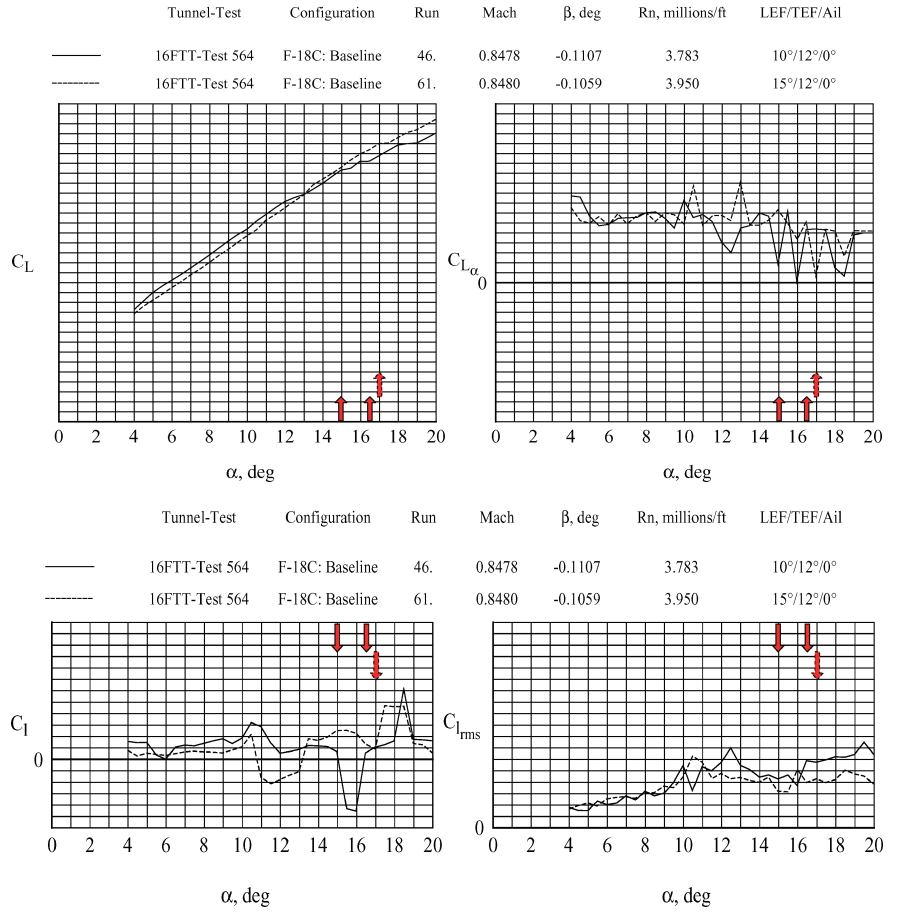

b) LEF/TEF/Ail at 10/12/0 and 15/12/0 deg

Fig. 8 Lift and rolling moments with FTR data for F/A-18C aircraft model at various flap settings and $M = 0.85$.

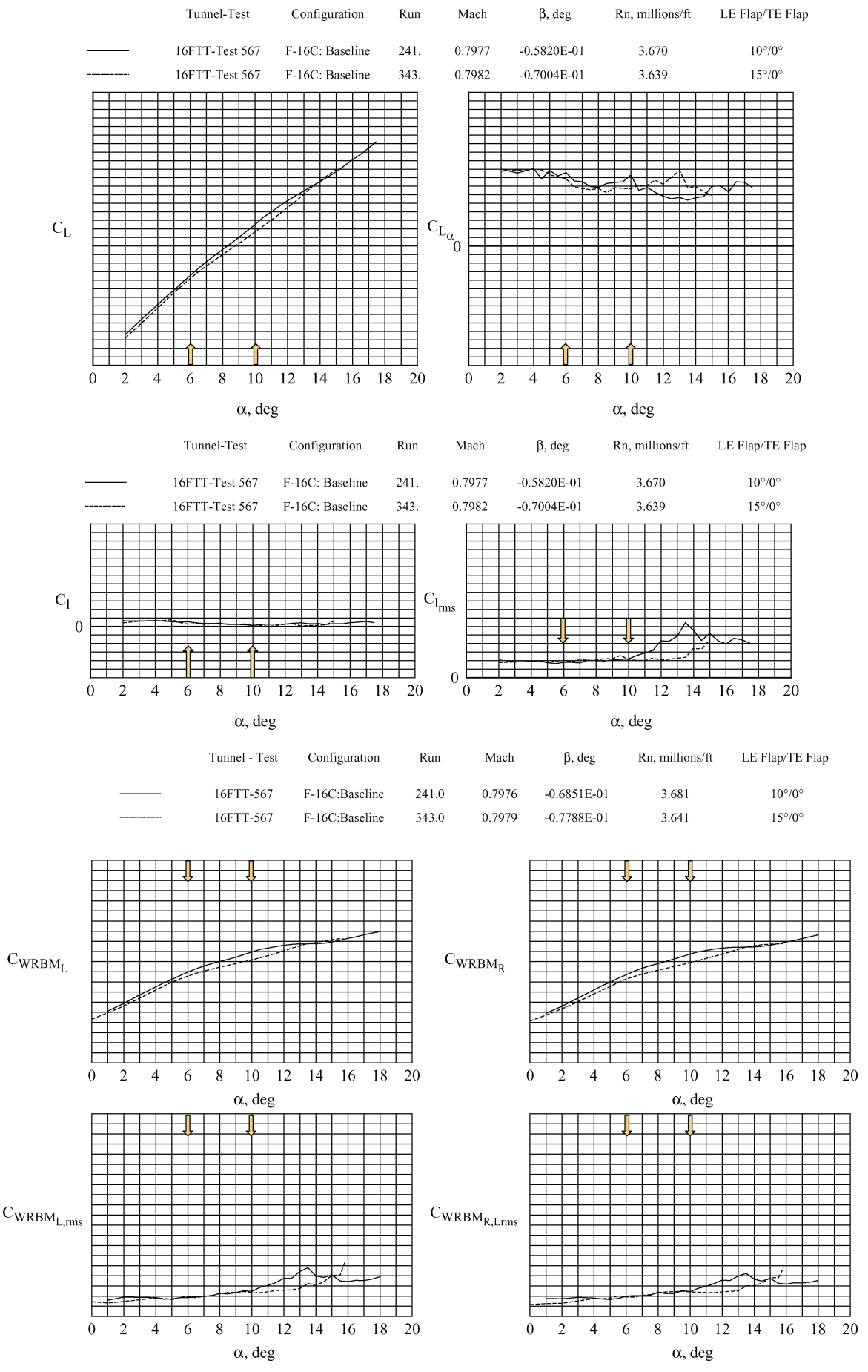

Fig. 9 Lift, rolling- and wing root-bending moments with FTR data for F-16C aircraft model at various flap settings and $M = 0.8$; LEF/TEF at 10/0 and 15/0 deg.

at values of α of 7, 9.5, and 10.5 deg, which produces agreement with four arrows and no misses for a score of 4(0)/5.

The $C_{\mathrm{WRBM,Rrms}}$ TFOM in Fig. 5b shows the solid curve to have an AWS rapid rise characteristic (envelope) for values of α from 7 to 10.5 deg and beginning again at 14 deg. Eight arrows have agreement and with no misses, and so the score for this curve is 8(0)/9. The dashed curve has AWS characteristics from 6.5 to 12 deg. Four of the arrows have agreement with no misses, yielding a score of 4(0)/5.

Example Results Summary

There are two general items worth noting from this example set of results. First is the rough equivalency between the number of single or group events/flags measured by both data sets. Second, for all of these TFOMs there are some values of α for which the static data lead the FTR data, whereas for others the reverse is true. Whether these statements hold true for all four configurations will be assessed after a review of Tables 1 and 2.

Data Comparison Presentations

The sample graphs in Figs. 6–9 are ordered by configuration, with those models associated with AWS events being first. Vertical scales on the graphs in Figs. 6–10 remain the same for each TFOM in this section. The test data reported are primarily from the most recent AWS tests, namely, 16FTT-563, -564, -565 and -567. There are some previously unreported data used here from 16FTT-523, the initial test of the preproduction F/A-18E model at NASA Langley Research Center. In an unpublished study, it was determined that the static data from test 16FTT-565 (the same model tested in the recent sequence) falls within the data repeatability of test 16FTT-523; hence, these data sets are used interchangeably. Figure 6 shows the F/A-18E preproduction 8% scaled model test at various leading-edge flap deflection angle, positive downward/trailing-edge flap deflection angle, positive downward/alleron deflection angle, positive down (LEF/TEF/Ail). The AV-8B 15% scaled model test is shown in Fig. 7 and the F/A-18C 6% scaled model test is shown in Fig. 8. The F-16C 1/15th scaled model test with FTR and static data is shown in Fig. 9.

Traditional FOMs: Ratings

Introduction of Tables 1 and 2

The results of the ratings (scorings) for each TFOM appear in Tables 1 and 2. Table 1 shows the details for each model, Mach number, and flap set. Table 2 summarizes all flap and Mach results into a single ratio for each configuration.

Discussion of TFOMs Ratings

The best score a TFOM could achieve in Tables 1 or 2 would be of the form 50(0)/50, which amounts to 100% agreement with no missed flags. Table 1 shows about half of the items to have 100% agreement, but only a small fraction of these have no misses. Table 2 generally shows a high percentage of agreement between the two data sets; however, it also shows that even with this agreement the TFOM $C_{L\alpha}$ has the largest number of misses of any parameter. The TFOMs with the fewest overall misses are the C_l, $C_{l,\mathrm{rms}}$, C_{WRBM} (excluding the F-16C data), and $C_{\mathrm{WRBM,rms}}$ terms. Even with good agreement overall, the TFOMs can give indications of FTR activity not validated by the response data, that is, false positives.

Discussion of TFOM Results

Three questions remain. 1) Can you rely on any TFOM to discern whether a new airplane model will experience an AWS event with certainty? This a restatement of the necessary and sufficient condition question raised earlier. 2) Does the TFOM data lead or lag the FTR response data? 3) Do any of these TFOMs help to sort the two sets of configurations into those that will likely have AWS events from those that are unlikely?

The answer to the first question is no, not with 100% certainty, based on these four model tests. Particular TFOMs indicate merely necessary conditions, but they are not always sufficient. The TFOMs can almost be considered conservative, yielding more flags than events; however they also miss events recorded by the FTR response data. Thus, if you can only employ one test technique to assess AWS events, use the FTR rig.

The answer to the second question is the same as stated in the "Example Results Summary" section. There appears to be no general pattern of one data type leading or lagging the other. The leading or lagging results are configuration, flap-set, and Mach number dependent. For example, with some combinations of models and Mach numbers, the $C_{L\alpha}$ data do indicate an increase in value followed by a decrease within an α range of 5 deg in the vicinity of the FTR arrows, whereas the opposite behavior is true for others.

In regard to third question about configuration sorting, an examination of the TFOMs in Figs. 3–9 (plus other figures not shown)[11] was made. The result is that all four models would be expected to have some AWS events based on the stringent criteria established. Thus, even though the TFOMs do not sort out the models perfectly, they are still very useful. Hence, all TFOMs should be employed in future tests to document those flagged features that have historically been associated with AWS events.

There is a related question. Did the FTR response data sort the models into two groups? Based on counting the arrows for each configuration, the answer is that this technique sorted three of the models, that is, the two known for AWS events, the preproduction F/A-18E and the AV-8B at the extremes of its flight envelope with the F/A-18C, flaps not on schedule, into the AWS group and the F-16C into the non-AWS group.

It is possible that other aerodynamic quantities, measured or derived from data collected during a static wind-tunnel test, may yet prove useful as FOMs.

Recommendations

There are four recommendations that can be drawn from a comparison of the static and FTR response data for these four fighter models. First, if possible, employ wing root-bending-moment gauges for each new model to help distinguish buffet from AWS events. Second, if the model is seen to be dynamically active during its initial testing at transonic speeds, then it is imperative that small α increments be taken in and around the α regions where the activity is noted. Third, examine all of the TFOM closely. In particular, the lift curve slope and the rolling-moment and wing root-bending-moment static and rms data can be meaningful indicators of a possible region of unwanted lateral flight activity. Close attention should be paid to those α ranges where there is a rapid change or excursion of a TFOM. Fourth, because the TFOM can give false positives with respect to AWS events, use the FTR rig.

Conclusions

This paper has examined TFOM for four current fighter aircraft models. The data used in these FOM were obtained from static testing of these models at transonic and subsonic speeds. There are two main themes in this paper. The first is whether there is a static FOM that is both a necessary and sufficient condition for predicting an AWS event as indicated by FTR response data. The result for the TFOM is no, not with 100% certainty. In particular, the TFOM indicate merely necessary conditions, but they are not always sufficient. Some of the TFOM, namely, the lift curve slope and the rolling-moment and wing root-bending-moment static and rms data, indicated potential AWS events for certain combinations of configurations and Mach numbers, but not all that had events. The TFOM can give false positives.

The second theme is whether an examination of the TFOM alone would sort the four models in groups of those likely to have AWS events and those unlikely. The result from this study is that all four models would be expected to have some AWS events based on the stringent criteria established. Thus, the TFOM did not sort out the chosen models from an AWS event perspective. This is of special importance when one remembers that the data processed did not take into account the flap schedule.

A corollary to the second theme is whether the static FOM or the FTR–FOM would show significant differences, in general, between the two configurations that exhibit wing drop and the two that did

not. As seen in Tables 1 and 2, there were not clear differences between the two wing droppers, the preproduction F/A-18E and the AV-8B at the extremes of its flight envelope, and the F/A-18C. This lack of distinction is not the result of any shortcomings in the FOM. Instead, the lack of distinction was because the F/A-18C would have been a very active dropper if its flap schedule had been different. That is, the lateral activity for the F/A-18C seen in the wind tunnel was at angles of attack higher than the angle of attack at which the aircraft flies for the given flap settings. This just underscores that a properly conceived flap schedule can avoid many flight handling-qualities problems, such as wing drop, which might otherwise occur. However, simply modifying flap schedule alone is not always sufficient to resolve these uncommanded motions, as was determined for the preproduction F/A-18E.

References

[1]Chambers, J. R., and Hall, R. M., "Historical Review of Uncommanded Lateral–Directional Motions at Transonic Conditions," *Journal of Aircraft*, Vol. 41, No. 3, 2004, pp. 436–447; also AIAA Paper 2003-0590, Jan. 2003.

[2]The Effects of Buffeting and other Transonic Phenomena on Maneuvering Combat Aircraft, AGARD-AR-82, Sect. 1.5.3, July 1975.

[3]Manoeuvre Limitations of Combat Aircraft, AGARD-AR-155A, Aug. 1979, p. 4.

[4]Capone, F. J., Owens, D. B., and Hall, R. M., "Development of a Free-To-Roll Transonic Test Capability," *Journal of Aircraft*, Vol. 41, No. 3, 2004, pp. 456–463; also AIAA Paper 2003-0749, Jan. 2003.

[5]McMillin, S. N., Hall, R. M., and Lamar, J. E., "Transonic Experimental Observations of Abrupt Wing Stall on an F/A-18E Model," AIAA Paper 2003-0591, Jan. 2003.

[6]Schuster, D. M., and Byrd, J. E., "Transonic Unsteady Aerodynamics of the F/A-18E at Conditions Promoting Abrupt Wing Stall," *Journal of Aircraft*, Vol. 41, No. 3, 2004, pp. 485–492; also AIAA Paper 2003-0593, Jan. 2003.

[7]Ross, A. J., "Flying Aeroplanes in Buffet," *Aeronautical Journal*, Vol. 81, Oct. 1977, pp. 427–436.

[8]Bore, C. L., "Post-Stall Aerodynamics of the Harrier GR1," *Fluid Dynamics of Aircraft Stalling*, CP-102, AGARD, 1972, p. 19-5.

[9]Owens, D. B., Capone, F. J., Hall, R. M., Brandon, J. M., Cunningham, K., and Chambers, J. R., "Free-to-Roll Analysis of Abrupt Wing Stall on Military Aircraft at Transonic Speeds," AIAA Paper 2003-0750, Jan. 2003.

[10]Capone, F. J., Hall, R. M., Owens, D. B., Lamar, J. E., and McMillin, S. N., "Recommended Experimental Procedures for Evaluation of Abrupt Wing Stall Characteristics," *Journal of Aircraft*, Vol. 41, No. 3, 2004, pp. 448–455; also AIAA Paper 2003-0922, Jan. 2003.

[11]Lamar, J. E., Capone, F. J., and Hall, R. M., "AWS Figure of Merit (FOM) Developed Parameters from Static Transonic, Model Tests," AIAA Paper 2003-0745, Jan. 2003.